Tunable all optical delay via slow and fast light propagation in a Raman assisted fiber optical parametric amplifier: a route to all optical buffering

David Dahan and Gadi Eisenstein

Electrical Engineering Department, Technion, Haifa 32000, Israel
ddahan@tx.technion.ac.il

Abstract: We propose and demonstrate the use of narrow band optical parametric amplification for tunable slow and fast light propagation in optical fibers. The parametric gain is coupled to the Raman process which changes the gain value moderately but modifies the gain spectral shape. Consequently, the delay is enhanced at short wavelengths while it is moderated at long wavelengths. The maximum delay and tuning range can be optimized with respect to each other considering saturation effects in long fibers. The proposed scheme offers tunable delay in the presence of gain and with a bandwidth which is sufficiently wide to process digital data streams at tens of Gbit/s rates as well as picoseconds pulses.

References and links

1. R.W. Boyd and D. J. Gauthier., "'Slow' and 'Fast' light ," Ch 6 in *Progress in Optics* **43**, E. Wolf, Ed. (Elsevier , Amsterdam, 2002), 497-530.
2. C.J. Chang-Hasnian, P.C. Ku, J. Kim, and S.L. Chuang, "Variable optical buffer using slow light in semiconductor nanostructures," in Proceedings of IEEE 91 **11**, 1884-1897 (2003).
3. L. V. Hau, S.E. Harris, Z. Dutton and C. H. Behroozi, "Light speed reduction to 17 metres per second in an ultracold atomic gas," Nature **397**, 594-598 (1999).
4. M. Xiao, "Novel linear and nonlinear optical properties of electromagnetically induced transparency systems," IEEE. J. Sel. Top. Quantum Electron. **9**, 86-92 (2003).
5. D. Strekalov, A.B. Matsko and L. Maleki, " Nonlinear properties of electromagnetically induced transparency in rubidium vapor," J. Opt. Soc. Am. B **22**, 65-71(2005).
6. P.C. Ku, F. Sedgwick, C.J. Chang-Hasnain, P. Palginis, T. Li, H.I. Wang, SW. Chang and SL. Chuang, "Slow light in semiconductor quantum wells," Opt. Lett. **29**, 2291-2293 (2004).
7. J. Mork, R. Kjaer, M. van der Poerl,L. Oxwenloewe and K. Yvind, "Experimental demonstration and theoretical analysis of slow light in a semiconductor waveguide at GHz frequencies," in Proceedings of CLEO 2005 Paper number CMCC5 (2005).
8. J. Kim, S.L. Chuang, P.C. Ku and C.J. Chang-Hasnian, "Slow light using semiconductor quantum dots," J. Phys. **16**, S3727-S3735 (2004).
9. R.S. Tucker, P.C. Ku and C.J. Chang-Hasnain, "Delay –bandwidth product and storage density in slow-light optical buffers," Electron. Lett. **41**, 208-209 (2005).
10. K.Y. Song ,M. Gozales Herraez and L. Thevenaz, " Observation of pulse delaying and advancement in optical fiber using stimulated Brillouin scattering," Opt. Express **13**, 82-88 (2005). http://www.opticsexpress.org/abstract.cfm?URI=OPEX-13-1-82
11. Y. Okawachi, M.S. Bigelow, J.E. Sharping ,Z.M.A. Schweinsberg, D.J. Gauthier, R.W. Boyd and A.L. Gaeta, " Tunable all-optical delays via Brillouin slow light in an optical fiber," Phys. Rev. Lett. **94** Art. No. 153902 (2005).
12. J.E. Sharping, Y. Okawachi, J. van Howe, C. Xu and A. Gaeta, " All-optical tunable, nanosecond delay using wavelength conversion and fiber dispersion," in proceedings of CLEO'05, paper CTuT1 (2005).
13. H Kidorf, K. Rottwitt, M. Nissov, M. Ma and E.Rabarijaona, " Pump interactions in a 100-nm bandwidth Raman amplifier," IEEE Photonics Technol. Lett. **11**, 530-532 (1999).

14. D. Dahan and G. Eisenstein, "The properties of amplified spontaneous emission noise in saturated fiber Raman amplifiers operating with CW signals," Opt. Commun. **236**, 279-288 (2004).
15. M.C. Ho, K. Uesaka, M. E. Marhic, Y. Akasaka, L. G. Kazovsky, " 200 nm bandwidth fiber optical amplifier combining parametric and Raman gain" J. Ligthwave Technol. **19**, 977-999 (2001).
16. D. Dahan , A. Bilenca and G. Eisenstein, "Noise optical reduction capabilities of a Raman mediated wavelength converter," Opt. Lett. **28**, 634-636 (2003).
17. K. Inoue and T. Mukai, "Experimental study on noise characteristics of a gain-saturated fiber optical parametric amplifier," J. Lightwave Technol. **20**, 969-974 (2002)**.**
18. J. Hansryd, P. A. Andrekson, M. Westlund, L. Lie and P.O. Hedekvist, "Fiber-based optical parametric amplifiers and their applications ," IEEE. J. Sel. Top. Quantum Electron. **8**, 506-520 (2002).
19. D. Dahan, E. Shumakher and G. Eisenstein, "A self starting ultra low jitter pulse source using coupled optoelectronic oscillators with an intra cavity fiber parametric amplifier," Opt. Lett. **30,** 1623-1625 (2005).
20. M. E. Marhic, K.K.Y. Wong and L.G. Kazovsky, "Wide-band tuning of the gain spectra of one pump fiber optical parametric amplifiers," IEEE. J. Sel. Top. Quantum Electron**. 10**, 1133-1141 (2004).
21. G. P. Agrawal, "Nonlinear Fiber Optics" 2nd Ed., (Academic Press, San Diego CA, 1995).

1. Introduction

Facing the exponential growth of the Internet traffic, next generation routers will be based on all optical technologies to scale their capacity to the traffic demand. Such routers will include all optical buffering functions which require in turn the development of new all optical tunable delay elements. A promising approach to an all optical variable delay uses non linear optics to control the velocity of optical pulses propagating through dispersive media - a concept that is termed slow and fast light [1-2]. The underlying principle of all slow and fast light schemes relies on using the highly dispersive nature of the group index in the spectral vicinity of a sharp absorption or gain resonance. Early demonstrations of slow light made use of electro magnetic induced transparency [3-5] in different media. Intense recent research is aimed at moving slow and fast light into the realm of potentially compact devices. For example, an approach to slowing light based on population pulsations in passive and active quantum wells [6-7] and in quantum dots [8] has recently been proposed but these have some fundamental limits related to the carrier life time [7].

Optical fibers enable trivial solutions (with linear pulse propagation) for discrete delay values. Operation in the nonlinear regime can add a continuous (and tunable) delay which covers the gaps between delay ranges thereby enabling a key building block of a potential optical buffer. Fibers have several advantages including a broad range of operating wavelengths, operation at room temperature and flexible lengths. Above and beyond that, nonlinear fibers offer gain over a band whose spectral shape is controllable. The gain spectrum functional shape and its bandwidth are related to the achievable delay [9] and therefore its controlled variability is an important advantage.

The first demonstration of slow light in optical fibers used the narrow gain bandwidth associated with stimulated Brillouin scattering (SBS) and achieved impressive results [10-11]. The disadvantage of SBS is of course its extremely narrow bandwidth which does not allow for narrow pulses to be delayed. A hybrid approach employing wavelength conversion by four wave mixing (FWM) followed by simple linear dispersion has also been suggested [12].

This paper reports on the first demonstration of slow and fast light in optical fibers based on the coupling of two nonlinear effects: narrow band partially degenerated optical parametric amplification (OPA) and stimulated Raman scattering (SRS). Both effects have been used extensively in the past for amplification [13-15] as well as for all optical processing devices like wavelength converters with reshaping capabilities [16-17] and ultra fast optical pulse sources [18-19]. The narrow gain spectrum needed for the controllable delay is mainly provided by the OPA, similarly to the scheme used as a tunable amplifying filter in multi channel communication systems [20]. The process of SRS has a relatively small effect on the obtainable gain; however, it modifies the gain spectral shape and therefore impacts

significantly the resulting delay. The entire process is termed therefore slow and fast light via SRS assisted OPA.

The proposed system has several advantages. First, it offers sufficiently wide bandwidths to enable the processing of digital data streams at tens of Gbit/s rates as well as picosecond pulses. Second, it offers large gain levels and therefore allows for the use of long fibers, in contrast to systems based on absorption resonance where the device length is limited by severe signal amplitude attenuation. The long fibers yield large delays together with large tuning ranges even though the group index change is moderate. The fundamental limiting factor of the proposed system is pulse distortion which originates from the dispersive nature of the group index (a phenomenon common to all slow and fast light systems) as well as from saturation of the parametric gain. A more practical limitation in the present system is the variation of the zero dispersion wavelengths along imperfect fibers.

We describe a theoretical analysis and experimental confirmations of controllable tuning of the delay experienced by a 70 ps wide pulse propagating in several lengths of dispersion shifted fiber (DSF) and assess the relationship between fiber length, maximum delay and tuning range. The interaction between OPA and SRS leads to a complex dependence of the delay on fiber length and gain. This dependence is modeled in detail and the results fit well to experiments. For a 500 m long fiber, the delay could be tuned continuously between 27.7 ps and 68.3 ps while for a 1000 m long fibers the delay range was 55 ps to 121 ps. A 2000 m long fiber offered the largest delay; 162 ps but the tuning range was reduced to 39.1 ps. Negative delays which amount to fast light were also demonstrated.

2. System set up

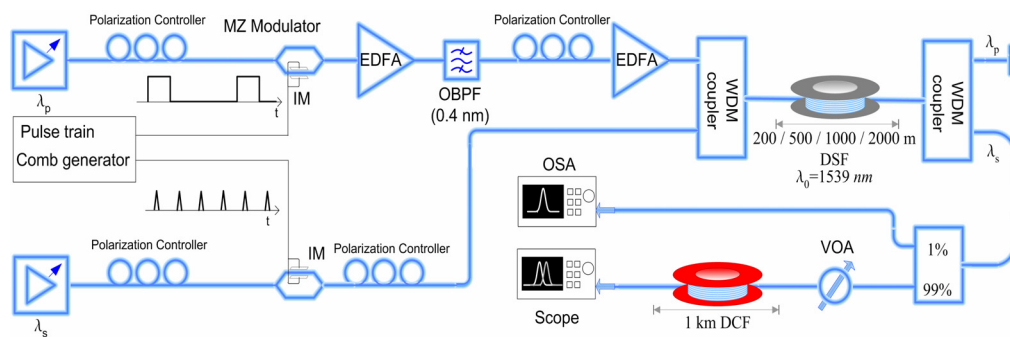The system we report is described schematically in Fig. 1.

Fig. 1. system set up : MZ (Mach Zendher), IM (Intensity modulation), EDFAs (Erbium Doped Fiber Amplifiers), OBPF (Optical Band Pass Filter), OSA (Optical Spectrum Analyzer)

A pulsed tunable laser source at λ_p (2 ns pulses at a duty cycle varying from 0.7% to 2.5%) serves as a pump source. It is pre-amplified and filtered before being further amplified by a high power amplifier with a maximum average output power of +27 dBm which amounts to a peak pulse power of a few Watts. A weak signal at λ_s is modulated to provide 70 ps pulses at 500 MHz and is combined with the pump wave through a WDM coupler. The two signals feed different lengths of DSF with an average zero dispersion wavelength λ_0=1539 nm and a negative fourth order dispersion coefficient β_4. As the pump wave propagates in the normal dispersion regime of the fiber, it generates, through a parametric process, symmetric narrow band gain spectra far from the pump wavelength [20]. The spectral separation between this narrow gain spectrum and λ_p increases while its width decreases as the spectral separation λ_0-λ_p increases. The parametric process is coupled to SRS for $|\lambda_p$-$\lambda_s|$ up to 150 nm enhancing the ability to tailor the shape of the gain spectrum with the pump power. Once λ_s falls within the narrow gain spectrum, it experiences gain and a change in the group index. At the same time, an idler wave is generated at λ_i.

A WDM coupler separates the waves at the DSF output. In order to remove the residual pump and idler waves at the signal port, we used a 1 km long Dispersion Compensating Fiber (DCF) which improves the temporal separation during the characterization. A Variable Optical Attenuator (VOA) was placed before the DCF to prevent nonlinear effects. An optical spectrum analyzer was used to map out the parametric gain spectra while a 10 GHz receiver followed by a sampling oscilloscope was employed for the characterization of the delay. The delay is obtained by comparing the temporal position of the pulse peak for various pump powers.

3. Theoretical analysis

The development of the parametric gain stems from the interaction among three complex fields $A_p(z,t)$, $A_s(z,t)$ and $A_i(z,t)$ representing the pump, signal and idler, respectively. Each of the fields (A_x) is formulated as in [18]: $A_x(z,t) = A_x(z)\exp\{i[k(\omega_x)z - \omega_x t]\}$. The fields have angular frequencies ω_p, ω_s and ω_i satisfying $2\omega_p = \omega_s + \omega_i$. With this formalism, it is sufficient to solve the coupled nonlinear Schrödinger equation (NLSE) for the z dependent field envelope $A_x(z)$. For negligible losses, the NLSE set is:

$$\begin{cases} \dfrac{\partial A_p}{\partial z} = j\gamma\left(\left|A_p\right|^2 + 2\left|A_s\right|^2 + 2\left|A_i\right|^2\right)A_p + j2\gamma A_p^* A_s A_i \exp(j\Delta k z) \\[2mm] \dfrac{\partial A_s}{\partial z} = j\gamma\left(2\left|A_p\right|^2 + \left|A_s\right|^2 + 2\left|A_i\right|^2\right)A_s + j\gamma A_p^2 A_i^* \exp(-j\Delta k z) - \dfrac{g_R}{2}\left|A_p\right|^2 A_s \\[2mm] \dfrac{\partial A_i}{\partial z} = j\gamma\left(2\left|A_p\right|^2 + 2\left|A_s\right|^2 + \left|A_i\right|^2\right)A_i + j\gamma A_p^2 A_s^* \exp(-j\Delta k z) + \dfrac{g_R}{2}\left|A_p\right|^2 A_i \end{cases} \quad (1)$$

where γ is the fiber nonlinear parameter, $\Delta k = k_i + k_s - 2k_p$, is the mismatch between the relevant propagation constants and g_R is the Raman gain coefficient ($g_R > 0$ for $\lambda_s < \lambda_p$ and $g_R < 0$ otherwise).

In the undepleted pump regime, $P_0 = \left|A_p\right|^2 \gg \max\left(\left|A_s\right|^2, \left|A_i\right|^2\right)$ and the pump wave envelope is given by:

$$A_p(z) = \sqrt{P_0}\exp(j\gamma P_0 z) \quad (2)$$

The coupled NLSE governing the signal and idler wave can be simplified:

$$\begin{cases} \dfrac{\partial A_s}{\partial z} = j2\gamma P_0 A_s + j\gamma P_0 A_i^* \exp\left(j(2\gamma P_0 - \Delta k)z\right) - \dfrac{g_R}{2}P_0 A_s \\[2mm] \dfrac{\partial A_i}{\partial z} = j2\gamma P_0 A_i + j\gamma P_0 A_s^* \exp\left(j(2\gamma P_0 - \Delta k)z\right) + \dfrac{g_R}{2}P_0 A_i \end{cases} \quad (3)$$

Eq. (3) can be rewritten using complex equivalent parameters g_s and g_i defined as:

$$\begin{cases} g_s = j\gamma\dfrac{P_0 A_i^*}{A_s}\exp\left(j(2\gamma P_0 - \Delta k)z\right) - \dfrac{g_R}{2}P_0 \\[2mm] g_i = j\gamma\dfrac{P_0 A_s^*}{A_i}\exp\left(j(2\gamma P_0 - \Delta k)z\right) + \dfrac{g_R}{2}P_0 \end{cases} \quad (4)$$

The real parts of g_s and g_i are related to the gain while their imaginary parts cause phase shifts in both waves leading to a change in the group index:

$$\Delta n_g = c \left(\frac{d \, \mathrm{Im} \left(g_{s,i} \right)}{d \omega} \right) \tag{5}$$

These variations of the group index lead to an optical time delay:

$$\Delta T = \int_0^L \frac{\Delta n_g \left(z \right)}{c} dz \tag{6}$$

where c is the speed of light in vacuum and L is the fiber length.

Eq. (3) yields analytical solutions for the signal and idler waves, as in [15]:

$$\begin{cases} A_s(z) = A_s(0) \left(\cosh(gz) + \left(-\frac{g_R}{2} P_0 + j \left(\gamma P_0 + \frac{\Delta k}{2} \right) \right) \frac{\sinh(gz)}{g} \right) \exp \left(-j \left(\frac{\Delta k - 2\gamma P_0}{2} \right) z \right) \\ A_i(z) = \frac{j\gamma P_0}{g} A_s^*(0) \sinh(gz) \exp \left(-j \left(\frac{\Delta k - 2\gamma P_0}{2} \right) z \right) \end{cases} \tag{7}$$

with

$$g^2 = \left\{ \left(\gamma P_0 \right)^2 - \left(\gamma P_0 + \frac{\Delta k}{2} \right)^2 + g_R P_0 \left(\frac{g_R P_0}{4} - j \left(\gamma P_0 + \frac{\Delta k}{2} \right) \right) \right\} \tag{8}$$

The complex nonlinear parameters g_s and g_i can be calculated from Eqs. (4) and (7)

$$g_s(z) = \frac{\left(\gamma P_0 \right)^2}{g} \frac{\sinh(gz)}{\left(\cosh(gz) + \left(-\frac{g_R}{2} P_0 + j \left(\gamma P_0 + \frac{\Delta k}{2} \right) \right) \frac{\sinh(gz)}{g} \right)} - \frac{g_R}{2} P_0 \tag{9}$$

$$g_i(z) = g \frac{\cosh(gz)}{\sinh(gz)} + j \left(\gamma P_0 + \frac{\Delta k}{2} \right) \tag{10}$$

When SRS does not play a significant role ($|\lambda_p - \lambda_s| > 150$ nm), simpler expressions are obtained for Eqs. (8) and (9):

$$g^2 = \left\{ \left(\gamma P_0 \right)^2 - \left(\gamma P_0 + \frac{\Delta k}{2} \right)^2 \right\} \tag{11}$$

$$g_s(z) = g_s^r(z) + j g_s^i(z) \tag{12}$$

with

$$g_s^r = \frac{\frac{\left(\gamma P_0 \right)^2}{g} \sinh(gz) \cosh(gz)}{1 + \left(\frac{\gamma P_0}{g} \sinh(gz) \right)^2} \tag{13}$$

$$g^i_s = -\frac{\left(\gamma P_0 + \frac{\Delta k}{2}\right)\left(\frac{\gamma P_0}{g}\sinh(gz)\right)^2}{1 + \left(\frac{\gamma P_0}{g}\sinh(gz)\right)^2} \tag{14}$$

A significant parametric gain is obtained as usual for frequencies satisfying $-4\gamma P_0 < \Delta k < 0$ [20]. When the pump wavelength is close to λ_0 in the normal dispersion regime, the phase matching condition occurs far from the pump wavelength and requires β_4 to be negative since:

$$\Delta k = \beta_2 \left(\omega - \omega_p\right)^2 + \beta_4 \left(\omega - \omega_p\right)^4 / 12 \tag{15}$$

This is illustrated is Fig. 2 where propagation constant mismatch is plotted as function of the frequency detuning in a 200 m long DSF with $\lambda_p = 1530$ nm, $\beta_2 = 8.73 \ 10^{-28}$ s^2/m and $\beta_4 = -5.6 \ 10^{-55}$ s^4/m at λ_p. For $P_0 = 10$ W, phase matching conditions are satisfied for frequencies corresponding to Δk values between the two dashed lines. Two narrow gain spectra, both located far from the pump frequency, are obtained at 1377 nm and at 1721.5 nm.
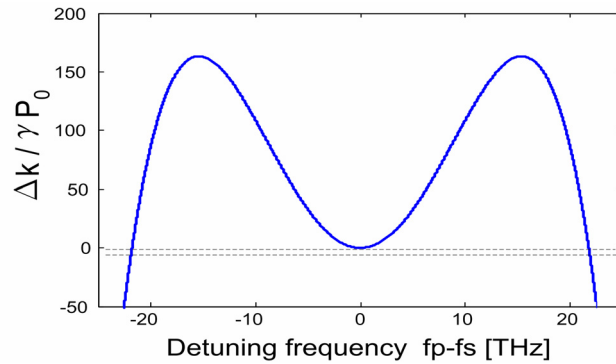

Fig. 2. Phase mismatching as a function of detuning for $\beta_2 = 8.73 \ 10^{-28}$ s^2/m and $\beta_4 = -5.6 \ 10^{-55}$ s^4/m at $\lambda_p = 1530$ nm

For large parametric gain values, Eq. (14) becomes :

$$g^i_s \approx -\left(\gamma P_0 + \frac{\Delta k}{2}\right) \tag{16}$$

And hence, according to Eq. (5), the change in the group index is for larger gain values is:

$$\Delta n_g \approx -\frac{c}{2}\frac{d\Delta k}{d\omega} = -c\left(\beta_2\left(\omega - \omega_p\right) + \beta_4\left(\omega - \omega_p\right)^3 / 6\right) \tag{17}$$

Equation (17) and Fig. 2 suggest that the narrow gain spectrum induces an increase of the group index for wavelengths shorter than the pump wavelength whereas it decreases the group index for wavelengths longer than the pump wavelength. It is to note that since the parametric process is coherent, slow and fast light are obtainable in both dispersion regimes provided that β_2 and β_4 have opposite signs. This is in clear contrast with the case where fast light propagation is induced by absorption when using stimulated Brillouin scattering [10].

Figure 3 shows calculated gain spectra and the resulting timing delay for wavelengths around 1337 nm (Fig.3(a)) and 1721.5 nm (Fig. 3(b)) with the pumping conditions that were used to calculate Fig. 2. The fiber length is 200 m. In both spectral regimes, the gain reaches

the same maximum value of 34 dB and the maximum absolute value of the induced timing delay is 19 ps. As explained previously, the timing delay is positive for the spectrum centered near 1377 nm while it is negative for the one at 1721 nm. Both delay spectra are large and quite flat over some 40 GHz where the gain exceeds 25 dB.
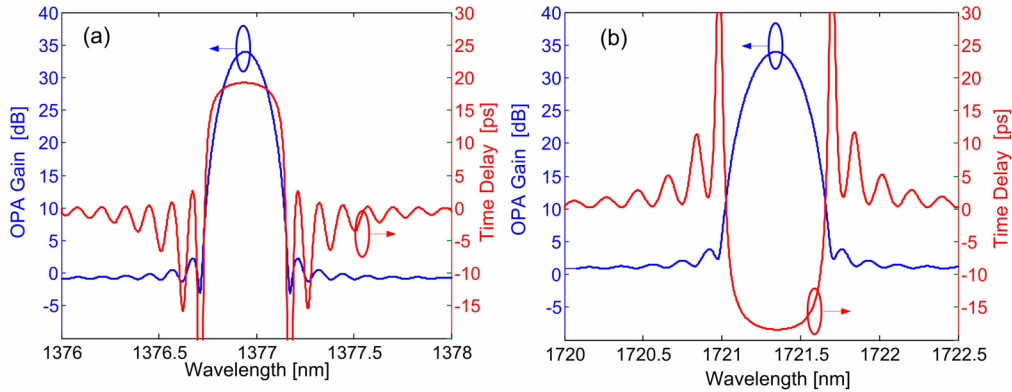

Fig. 3. Calculated OPA gain and induced time delay spectra at (a) the short and (b) long wavelength region using a 200 m long DSF for β_2=8.73 10^{-28} s^2/m and β_4=-5.6 10^{-55} s^4/m at λ_p=1530 nm

When the wavelength separation between the signal and the pump is less than 150 nm, SRS becomes significant introducing an asymmetry between the local gain parameter values at short and long wavelengths. The parameter g is complex in this case with the expression describing the group index becoming cumbersome so that it can only be calculated by solving Eqs. (5) and (9) numerically. When the phase matching conditions are not satisfied, the Raman effect causes a signal whose wavelength is shorter than that of the pump to experience attenuation while a signal whose wavelength is longer than the pump wavelength is amplified. For phase matched conditions, the Raman effect changes slightly the OPA gain, reducing it at short wavelengths and increasing it at long wavelengths [15]. OPA gain occurs therefore at short wavelengths with the background of Raman induced absorption and hence the complex parameter g_s has sharper transitions, leading to a larger group index change and to an enhancement of the time delay. On the other hand, with a signal wavelength longer than the pump wavelength, the OPA gain adds to an already Raman amplifying spectral region which softens the transition of g_s, leading to a lower group index change and therefore a smaller time delay.
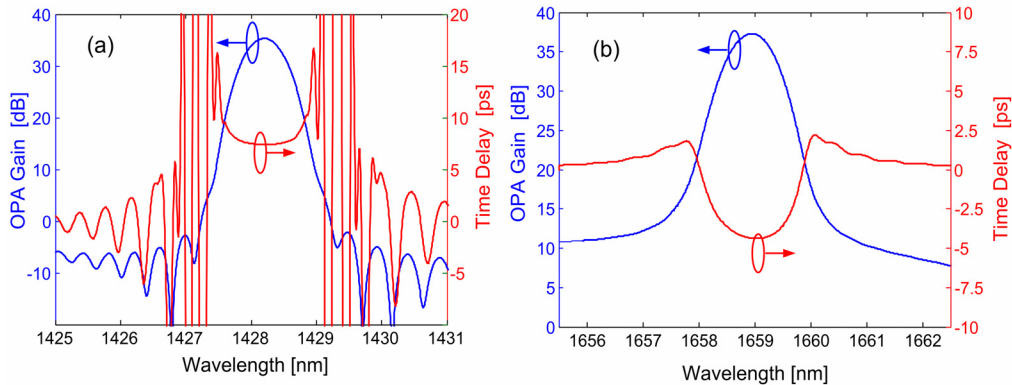

Fig. 4. Calculated Raman assisted OPA gain and induced time delay spectra at the (a) short and (b) long wavelength region using a 200 m long DSF for β_2=3.95 10^{-28} s^2/m and β_4=-5.7 10^{-55} s^4/m at λ_p=1535 nm

The role of the Raman effect is illustrated in Fig. 4 which exhibits calculated gain spectra and the resulting timing delay in a 200 m long DSF for wavelengths around 1428 nm (Fig.4(a)) and 1659 nm (Fig 4(b)). The pump wavelength is λ_p=1535 nm and the fiber parameters are β_2=3.95 10^{-28} s^2/m and β_4=-5.7 10^{-55} s^4/m at the pump wavelength. The Raman effect introduces an asymmetry to the spectra resulting in maximum gain values of 33 dB and 37 dB at the short and long wavelengths, respectively for P_0=10 W. The time delay is larger in the short wavelength region, especially at the edges of the gain spectrum. The obtained delay is 7.5 ps over a fairly flat region for gain values larger than 25 dB, which represents an operational bandwidth of 150 GHz. In the long wavelength region, the time delay within the gain spectrum is negative (namely the velocity is increased) and smaller reaching a constant value of -4.5 ps over 110 GHz where the gain is larger than 30 dB.

The impact of the Raman effect on the obtainable delays is further demonstrated in Fig. 5 which shows the gain and delay spectra for the same pump wavelength as in Fig. 4 but with the Raman effect omitted from the calculation. The gain spectra are symmetric once more and the obtained delays differ from Fig. 4. The absolute delay values become 5.4 ps in both spectral regions. Comparing Fig. 5 and Fig. 3 (both having no Raman contribution) shows that indeed when the pump wavelength is longer, the gain spectra are broader and the delay is reduced.
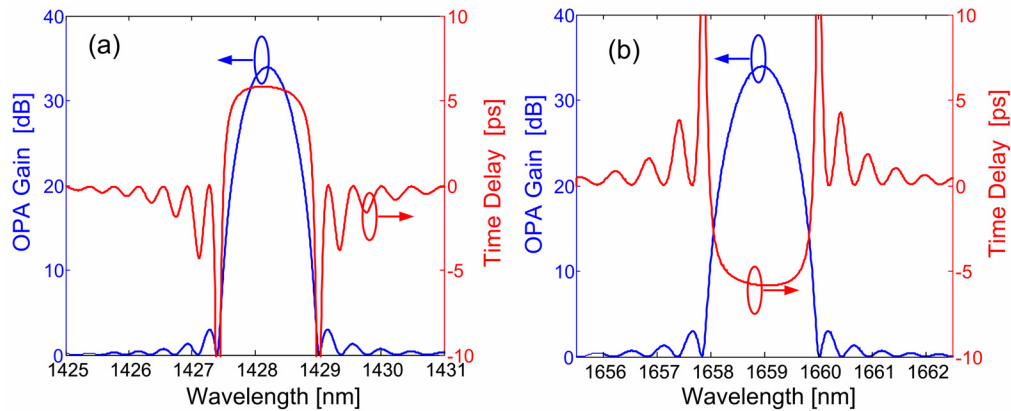

Fig. 5. Calculated OPA gain and induced time delay spectra with the Raman effect omitted artificially. (a) short and (b) long wavelength region using a 200 m long DSF with for β_2=3.95 10^{-28} s^2/m and β_4=-5.7 10^{-55} s^4/m at λ_p=1535 nm

It is important to note that slow and fast light are defined in Fig. 3 to Fig. 5 for the signal only. Namely, for a given pump wavelength, the signal experiences slow light at the short wavelength gain spectrum and fast light at the long wavelength gain spectrum. In either case, the idler propagates at essentially the same velocity as the signal

4. Measured Raman assisted OPA spectra

Figure 6(a) describes measured amplified spontaneous emission (ASE) spectra in a 200 m long DSF for different values of λ_p. Shown are spectra on the short wavelength side of λ_p but a symmetric duplication exists at long wavelengths. These ASE spectra (which are similar to the ones given in [20]) represent the exact spectral shape of the Raman assisted parametric gain since the two are proportional to each other. The functional shapes of the gain spectra are in good agreement with theoretical calculations exhibited in Fig. 6(b). Each narrow gain spectrum induces a group index change leading to a delay which can be enlarged by sharpening the gain spectra via an increase of the detuning λ_0-λ_p. However, maintaining a constant peak gain value requires to increase the pump power as the spectral separation λ_0-λ_p widens. Some gain broadening and a reduction in efficiency occur in practical fibers due to

longitudinal variations of the zero dispersion wavelength. These effects are enhanced as the spectral separation becomes large.
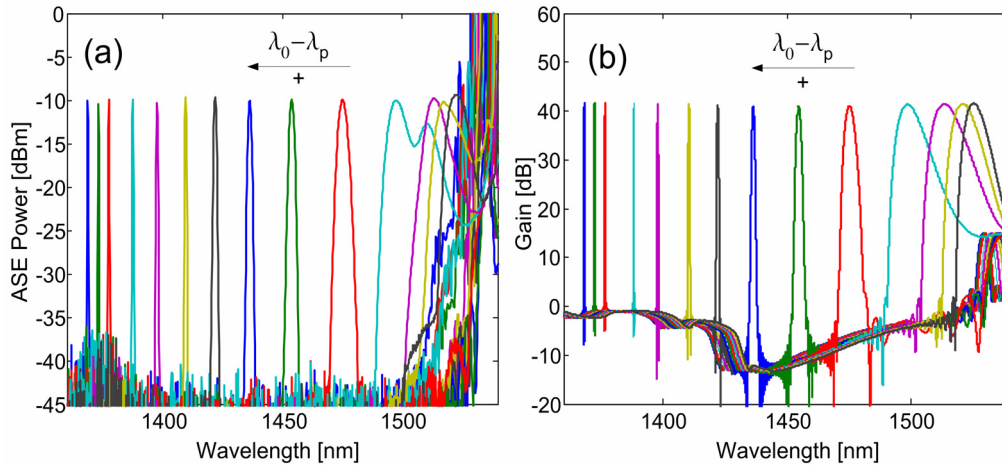

Fig. 6. (a) Experimental ASE power spectra and (b) Theoretical gain spectra for 200 m DSF using different pump wavelengths.

Figure 7(a) shows a zoom of measured ASE spectra centered around 1428 nm in a 200 m long DSF for different pump powers at a fixed λ_p of 1535 nm. The spectra width varies from 1 nm to 5 nm when the gain at λs=1428.6 nm increases from 25 to 49 dB. The spectra broaden and shift towards shorter wavelengths (since $\beta_4<0$) as predicted by the numerically calculated gain spectra in Fig. 7(b). The coupling between the parametric process and SRS widens the gain spectra especially on the short wavelength side while it slightly decreases the gain. This is clearly seen in Fig. 7(b) which also shows gain spectra with the Raman contribution omitted in the calculations. The somewhat wider experimental spectra are attributed once more to a longitudinal variation of λ_0 along the fiber. Furthermore, the increase in the pump power, needed to compensate for the gain efficiency reduction, enhances the SRS effect which causes a larger spectral broadening on the short wavelength side compared to theory.
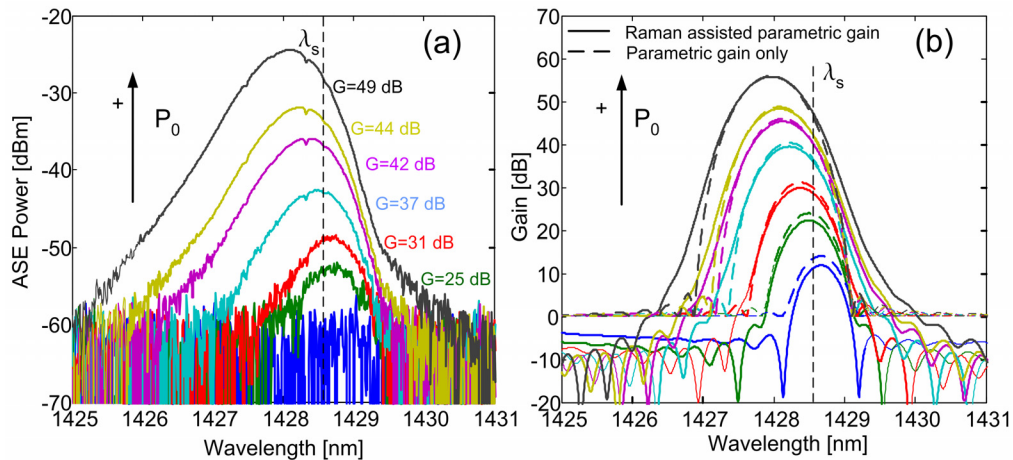

Fig 7. (a) Experimental ASE power spectra and (b) theoretical gain spectra for 200 m DSF using different pump power levels with λ_p=1535nm. The gain is evaluated at λ_s=1428.6 nm

5. Slow light observations

Slow light experiments were performed using the experimental set up shown in Fig. 1. In the first experiment, the fiber length was 200 m and the pump wavelength was λ_p=1536.3 nm. The signal wavelength was chosen to be λ_s=1448.8 nm. Figure 8(a) describes measured pulse positions for different gain levels. Figure 8(b) shows calculated results obtained by solving numerically the nonlinear Schrödinger equation [21].
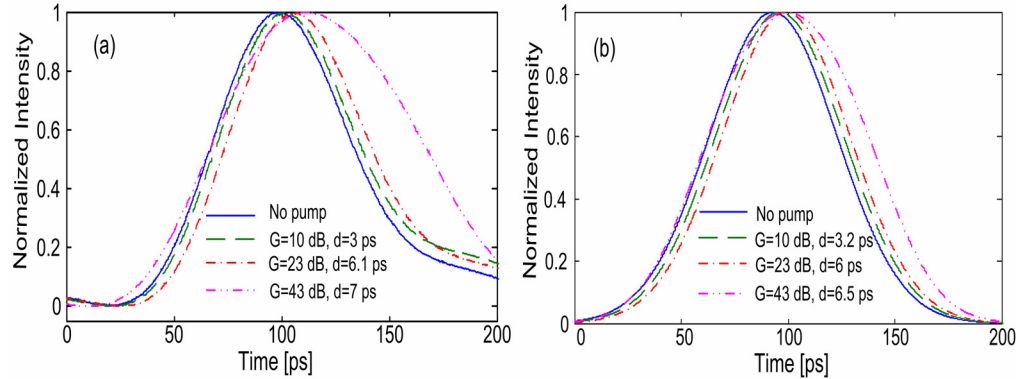

Fig 8. Pulse position for different gain values at λs=1448.8 nm using a 200 m long DSF (a) Experimental results (b) Simulated results

The simulation predicts the experimental results well. In both cases, the delay increases with gain reaching a value of 6.5 to 7 ps. This rather moderate delay value is a result of the short fiber and the small pump detuning from λ_0. As the gain increases and saturation effects start, the pulse broadens somewhat which is more apparent in the experimental results because of an asymmetry of the pulse used. The short fiber and the relatively broad gain spectrum minimize the detrimental effect of variation in λ_0 along the fiber enabling the good fit between experiments and simulations.

In order to demonstrate the delay dependence on fiber length and pump wavelength, a second experiment was performed with λ_p=1535 nm and λ_s=1428.6 nm. Several lengths of DSF between 200 m and 2 km and were used as shown in Fig. 9. Each group of curves in Fig. 9 compares the pulse temporal position with the pump turned off (trace (1)) to the corresponding pulse positions with varying levels of parametric gain. Table 1 summarizes the minimum and maximum delays and tuning ranges obtainable for each fiber length.

Table 1. Gain and delay values achieved at λ_s=1428.6 nm using different lengths of DSF

Fiber length [m]	200	500	1000	2000
Minimum gain, G_{min} [dB]	14.1	16.6	5.2	8.2
Minimum delay, d_{min} [ps]	10.2	27.7	55	122.4
Maximum gain, G_{max} [dB]	44	46.5	43.4	41
Maximum delay, d_{max} [ps]	21.2	68.3	121	161.5
Tuning range, Δd [ps]	11	40.6	66	39.1
$\Delta d/d_{min}$ [%]	108	146	120	32

In all cases, the delay increases with gain and with the fiber length. The maximum delay increases from 21.2 ps to 161.5 ps with the DSF lengths varying from 200 m to 2000m. For a fixed fiber length, a gain increase can cause the amplifier to saturate. The delay still increases in that case but some pulse width broadening may also occur.

Since the gain is nonlinear and also broadens with pump power, there is a minimum pump level for which the entire pulse spectrum is amplified. In the experiment, we define this minimum gain level as the lowest gain which ensures a properly detected signal with a

standard 10 GHz receiver. The maximum gain is defined as the largest gain at which a clear pulse shape is detected.
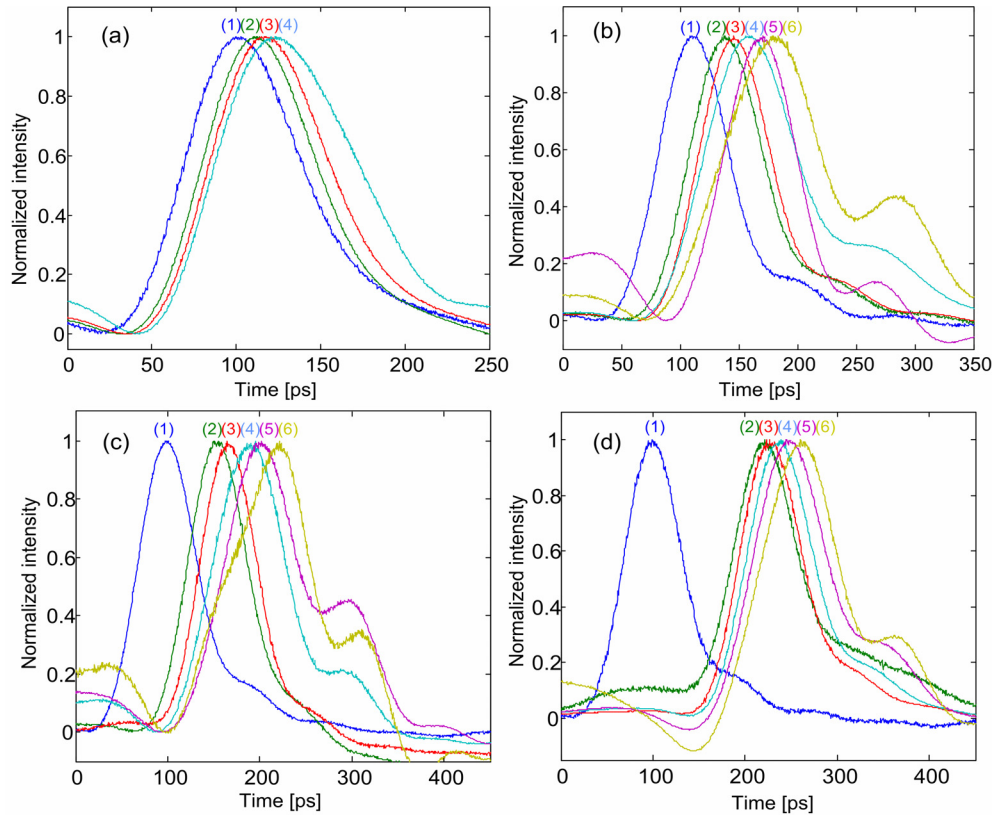

Fig 9. Experimental traces for different gain values at λ_s=1428.6 nm using different DSF lengths :(a) 200 m , (b) 500 m, (c) 1000m, (d) 2000 m The curves indexes represent different gain values which are summarized in Fig. 10

Figure 10 describes measured delays as a function of parametric gain for different fiber lengths.
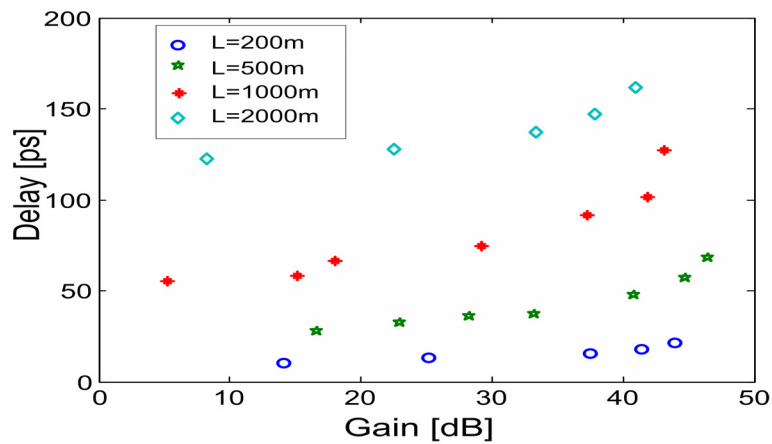

Fig. 10. Measured delay as a function of gain for different fiber lengths at λ_s=1428.6 nm

The results of Fig. 10 raise two issues. Firstly we note an interplay between maximum delay and tuning range. For a fixed gain level, the delay increases with fiber length. However, the obtainable delay range (relative to the minimum delay) decreases for very long fibers due to saturation. There exists therefore an optimal length which in the present experiments is 500 m where the tuning range is 1.46 times larger than the minimum delay.

A second, more subtle, issue relates to the dependence of delay on the gain level. The delay in Fig. 10 does not seem to converge to zero at low gain levels, in particular for long fibers. This behavior is due to the interplay between the Raman effect and the parametric gain, as described in the simulated results shown in Fig. 11.
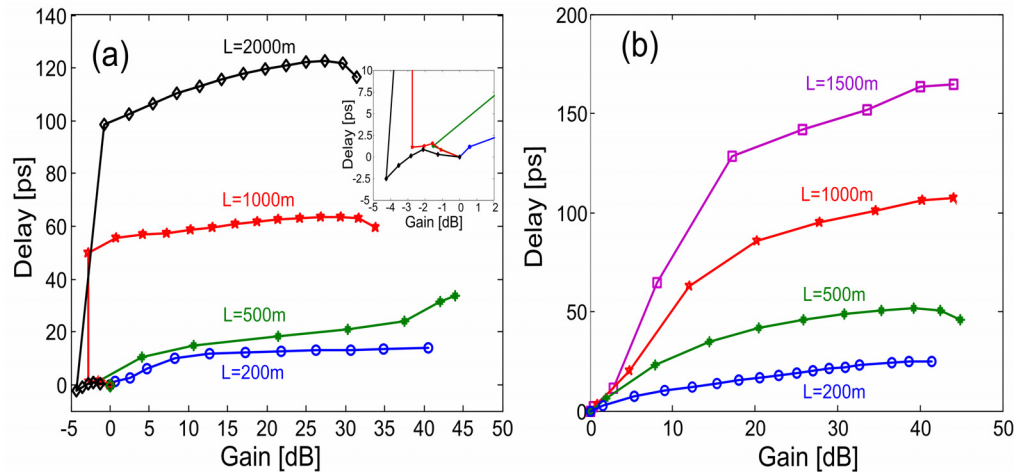

Fig. 11. Calculated delay as a function of gain for different fiber lengths. (a) λ_s=1428.6 nm, (b) λ_s=1377.1 nm

Figure 11(a) simulates the experiment described in Fig. 9 and Fig. 10. Each curve represents the evolution of gain and delay with an increasing pump power. For long fibers and small pump powers, the OPA gain is low and its spectrum is narrower than that of the pulse. The Raman spectrum is absorptive and broad band so that the overall gain is negative. The delay under those conditions is small and can be either positive or negative as seen in the insert. As the pump power increases, the OPA gain rises, broadens and shifts to short wavelengths (see Fig. 7). For this gain regime, parts of the pulse spectrum do not experience gain (leading to severe pulse distortions) and therefore the delay is ill defined. At some point the OPA gain band width becomes sufficiently large to amplify the entire pulse spectrum and the delay grows abruptly resulting in the threshold like behavior seen in Fig. 11(a). For short fibers, the OPA gain at low pump levels is wider so that the spectral filtering effect is negligible. For the 500 m fiber, the insert shows a trace of the threshold like behavior while at 200 m it is all but diminished. A quantitative comparison with Fig. 10 reveals a good agreement with some differences at large gain and long fibers. The measured data in Fig. 10 is for gain levels of 5 dB and more so that the absorptive regime is not seen. The differences between the experiments and the simulations are attributed to the variations of the zero dispersion wavelength along the imperfect DSF.

Figure 11(b) describes simulated delays for a large detuning where the Raman gain plays no role. Here the delay converges to zero at low gain and the fiber length determines the slope. The spectral filtering effect stemming from the narrow OPA spectral width in long fibers manifests itself in the changing slope for gain level as below 20 dB in the 1000 m and 1500 m cases. Note that the filtering effect is more severe here since the OPA spectral width decreases at short wavelengths (see Fig. 6). For fibers longer that 1500 m, the situation worsens as the OPA spectral width is much narrower than the pulse spectrum for all reasonable gain levels.

The exact relation between delay, fiber length and OPA gain is rather complex due to the distributed nature of the parametric gain. Figure 12(a) shows calculated gain spectra obtained using 200 m and 2000 m long DSF using the same pump wavelength. The two Raman assisted amplifiers provide the same gain level of 34 dB at λ_s=1428.6 nm. The long fiber was pumped with 1W and its gain spectrum peaked at λ_s. The short fiber was pumped with 16.75 W and its gain spectrum peaked at λ_{peak} = 1427.6 nm with a maximum level of 60 dB. The most noticeable feature is the spectral narrowing obtained by the longer fiber which stems from the limited wavelength range over which phase matching conditions are satisfied, consistent with [18].

Obviously, the gain spectral shape varies along the fiber and consequently, the group index varies continuously as described in Fig. 12(b). Shown are group index distributions at λ_s for both fibers as well as at the peak gain for the short fiber. In all cases, the group index varies linearly before reaching a plateau after some distance. The longer amplifier has a narrower spectrum but its pump level is lower and hence, the spectral gain level variations per unit length are smaller. The overall delay which is the accumulative effect of the group index distribution is larger in the long fiber as predicted by Eq. (6). The small tuning range of long fibers results from the fact that their minimum delay is large and they saturate rapidly. In the short amplifier, the signal is located at the gain spectrum edge where the group index variations are enhanced (an enhancement which does not take place near the gain peak)
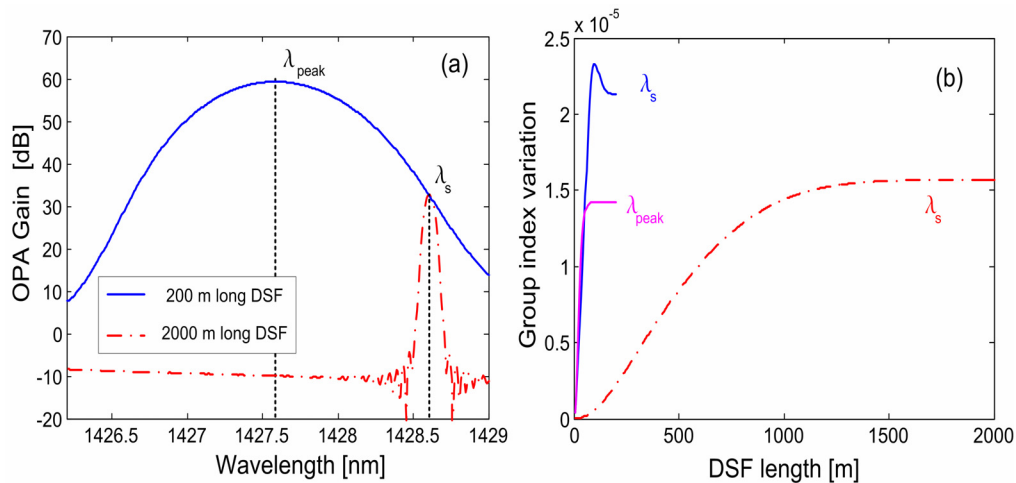

Fig. 12. (a) Theoretical gain spectra using 200 m and 2000 m long DSF, (b) Group index variations along the fiber at λ_s and λ_{peak}

The delay variations with the signal position across the gain spectrum were investigated using a 200 m long DSF. The short fiber was chosen in order to minimize the effect of longitudinal variation in λ_0. Due to a lack of tunable sources in the 1427 nm range, we kept the signal wavelength fixed at 1428.6 nm and varied the pump wavelength so as to sweep the gain spectrum across the signal. Since the required pump wavelength changes were small, the gain spectral shape remained unchanged.

Figure 13(a) shows measured ASE spectra for different pump wavelengths. Tuning the pump by only 0.18 nm enabled to completely scan one edge of the gain spectrum across the signal wavelength while the gain spectral shape remain unchanged. Figure 13(b) describes the corresponding measured time delays experienced by a pulse at the signal wavelength. As predicted by the theory, the combined effects of SRS and parametric gain enhance the time delay at the spectral edges while the gain is decreased. When the parametric gain does not completely compensate for the Raman induced absorption, the delay is increased by as much as a factor of three. A slight signal broadening is noticeable in two cases, however. When the

signal is close to the peak gain, broadening is caused by saturation while when it is located at the spectral edge, there are strong group index variations which induce dispersion
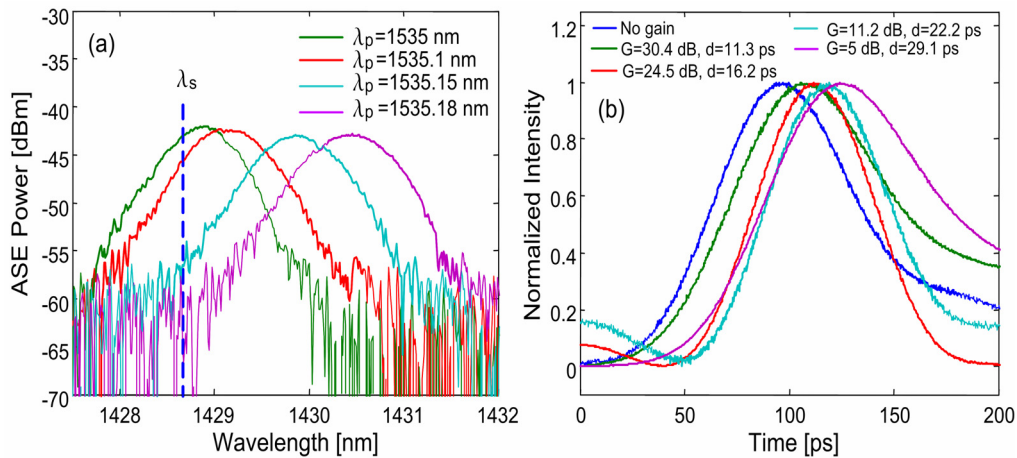

Fig. 13: (a) ASE power spectra for different pump wavelengths (b) The corresponding signals at λ_s=1428.6 nm

6. Fast light observations

Fast light (negative delay) occurs at wavelengths longer than the pump as explained in Section 3. The longest available wavelength from a single mode laser was λ_s=1600 nm where the induced negative delay per unit length is very small. In order to demonstrate the principle of fast light we used 2000 and 3000 m long DSF where Raman assisted OPA enabled observable pulse advancement. In order to provide gain at λ_s = 1600 nm, we set the pump wavelength at λ_p=1537.6 nm. The results are presented in Fig. 14.
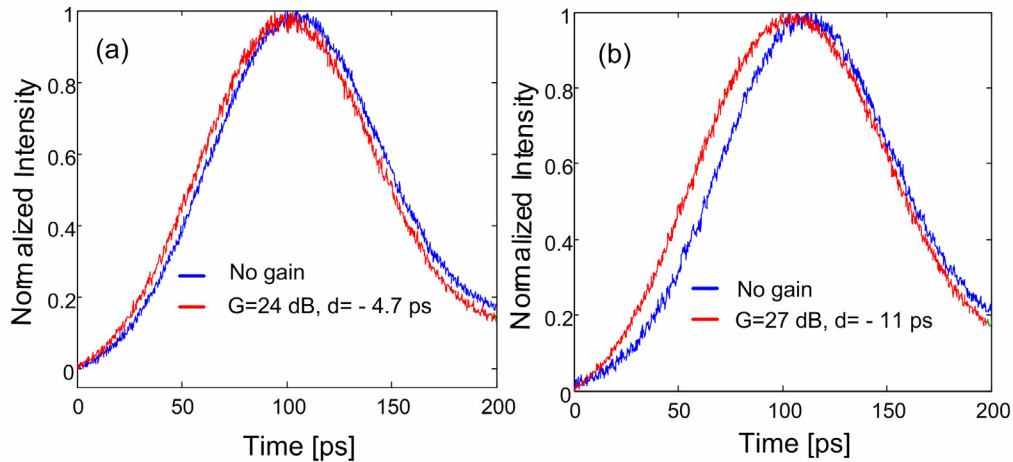

Fig. 14. Fast light observation at λ_s=1600 nm using (a) 2000 m long DSF (b) 3000 m long DSF

For a 2000 m long DSF, we obtained a pulse advancement of 4.7 ps for a gain of 24 dB and by using 3000 m long DSF, the advancement for a gain of 27 dB increased to 11 ps. However, for this latter case, the pulse undergoes some broadening which may result from a

combination of pump saturation and dispersion induced by the strong variation of the group index induces at the gain spectral edges.

The negative delay dependence on fiber length and gain was also addressed. Unlike the case of slow light, the Raman effect adds gain at low pump power and therefore the behavior is more intuitive. Figure 15 describes a calculation for small detuning (where the Raman effect is important) and large detuning where only the OPA gain affects the pulse. For the shorter wavelength (Fig. 15(a)), the spectral filtering effect is negligible because the OPA gain is fairly broad and the Raman effect adds to it. The dependence is therefore monotonic. For large detuning, where the OPA gain is the only physical mechanism affecting the pulse advancement (Fig. 15(b)), the spectral filtering sets in for long fibers, as is clearly apparent in the case of the 1500 m long fiber.
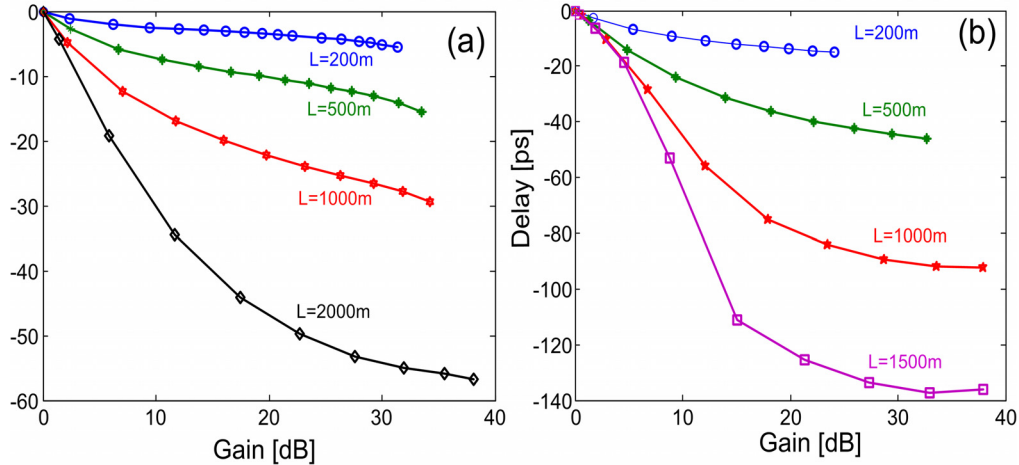
Fig. 15. Calculated negative delay as a function of gain for different fiber lengths. (a) λ_s=1658.3 nm, (b) λ_s=1721.1 nm

7. Conclusion

We have proposed and demonstrated, both theoretically and experimentally, pulse delay and advancement via slow and fast light propagation in optical fibers using Raman assisted OPA. Controllable narrow gain spectral shapes can be tailored by selecting the appropriate pump wavelength and power. The scheme requires operation in the normal dispersion regime of a DSF with a negative β_4 or in the anomalous dispersion regime when β_4 is positive. The narrow gain spectra induce a change in the group index of the fiber which is in the order of 10^{-5}. While this is quite a small change, it is accompanied by a large gain which enables the use long fibers which yield, in turn, long delays with no loss of signal due to attenuation. We demonstrate large delays and delay tuning ranges, on the order of 160 ps for a 70 ps wide pulse propagating in DSF with lengths up to 2000 m. The principle of fast light was also demonstrated. The lack of single mode sources at very long wavelengths prevented the achievement of large enhancements. Nevertheless, operation at 1600 nm with a 3000 m long DSF yielded a negative delay of 11 ps which is sufficient to prove the fast light capability.

The available bandwidth for slow and fast is tens to hundreds of GHz which allows for the delay of fast digital data signals as well as ps pulses. In fiber with negative β_4, slow light are observed at wavelengths shorter than the pump wavelength whereas fast light are observed at longer wavelengths. When the wavelength difference between the signal and the pump is less than 150 nm, SRS is combined with the parametric process. SRS enhances the group index variations when it induces signal absorption whereas it reduces them when inducing signal amplification.

The tunability of the delay or advancement is controlled by changing the amplifier gain or the pump wavelength. Longer fibers offer larger delays or advancements but this may be at the expense of the tuning range. An interesting property is the highly nonlinear dependence of delay on gain and fiber length when slow light is considered and when the Raman effect contributes. This results from the fact that a finite gain is needed in order to compensate for the Raman induced loss and to achieve a sufficiently wide gain bandwidth that overlaps the entire pulse spectrum. As in all slow and fast light techniques, pulse distortions set a fundamental performance limit. The ability to tailor the gain spectrum in the present system opens the possibility to effectively manage this undesired effect. A practical limitation is the longitudinal variation of the zero dispersion wavelength along the fiber which causes a decrease in the gain efficiency and broadens the gain spectra. These effects are enhanced when the gain spectra get narrower.

Acknowledgments